

6th International Conf. on Nitride Semiconductors
28 Aug - 2 Sept. 2005
Bremen, Germany.

Electrical characteristics and thermal stability of Ti contact to p-GaN

C. K. Tan, A. Abdul Aziz, Z. Hassan, F. K. Yam, A. Y. Hudeish.

School of Physics, Universiti Sains Malaysia, 11800 Minden, Penang, Malaysia.

Received zzz, revised zzz, accepted zzz

Published online zzz

PACS 73.30.+y, 73.61.Ey, 73.20.-r

The Schottky barrier height (SBH), Φ_B of the diodes were characterized by I-V-T method (energy activation plot and modified Norde plot) in the range of 300K-373K ambient for various annealing temperature (500-1000°C) in N_2 gas flow. The ratio of $kT/E_{oo} \approx 1$, large A^{**} and large deviation of X from general value indicate that the mixed thermionic emission with thermionic field emission are most possible to be occurred as current transport mechanism.

© 2004 WILEY-VCH Verlag GmbH & Co. KGaA, Weinheim

1 Introduction

Wide band gap GaN semiconductor has a variety of applications in optoelectronic devices such as light-emitting diodes and laser diodes [1]. In addition, its high electron saturation velocity, large breakdown field and thermally stable makes an attractive candidate for high temperature/high power devices. It has been shown that devices such as field-effect transistors (FETs) [2,3] can be fabricated on GaN. For high temperature operation of metal-semiconductor field-effect transistors (MESFETs), thermally stable Schottky contacts are necessary. The barrier height Φ_B is determined by the metal work function Φ_m , the band-gap E_g and the electron affinity χ of p-GaN and can be expressed as:

$$\Phi_B = (X + E_g) - \Phi_m \quad (1)$$

The above expression is valid for an ideal Schottky diode [4]. Despite its decisive role for improving device performance, electrical property of the p-type GaN layer, which differs much from the n-type layer due to the complicated behavior of Mg acceptors, has yet to be fully explored [5,6]. So far, only a few studies on this subject have been reported and the Schottky barrier heights (SBH) of various metal contacts are not well defined yet. In addition, little has been reported in the literature on the thermal stability of Schottky barrier contact [7,8].

In this work, the I-V-T characteristics of the contacts; as-deposited and annealed at 500-1000°C were investigated in the consecutive elevation temperatures of 20°C from room temperature to 373K. The SBHs of these contacts determined using current-voltage-temperature (I-V-T) measurements were calculated using activation energy plot.

2 Experimental

© 2004 WILEY-VCH Verlag GmbH & Co. KGaA, Weinheim

Mg-doped p-GaN samples grown on sapphire (Al_2O_3) substrates were used in this study. The ohmic metallization consists of a single layer of Ni (50nm) whereas; Ti (50nm) Schottky is used as single layer of Schottky contact. Prior to the metallization, conventional boiling aqua regia cleaning method was used to chemically etch and clean the samples. Ni was first formed on p-GaN to act as Ohmic contacts. This contact was checked and confirmed to be Ohmic by I-V measurement prior to the deposition of Schottky contact. Metallized dots, which consist of an array of dots with a diameter of 200 μm for Schottky contacts, were sputtered via a stainless steel metal mask onto the p-GaN samples. The annealed samples were conducted inversely to as-deposited sample, where Schottky contacts (Ti) were annealed in respect to selected temperature and duration of annealing prior to metallization of Ohmic contact. In this investigation, Schottky diodes were annealed at temperature ranging from 500-1000°C with the flow of N_2 gas. Digital hot chuck system was used to heat up the samples from 27-100°C and the I-V-T characteristics of Ti/p-GaN Schottky diodes was analyzed using standard semiconductor parameter analyzer.

3 Result and discussion

The electrical parameters, i.e., SBHs, Φ_B , saturation current, I_o , and ideality factor, η can be determined by I-V measurements. For thermionic emission and $V > 3kT/q$, the general diode equations are [9]:

$$I = I_o \exp\{qV/\eta kT\} \quad (2)$$

$$I_o = AA^*T^2 \exp\{-q\Phi_B/kT\} \quad (3)$$

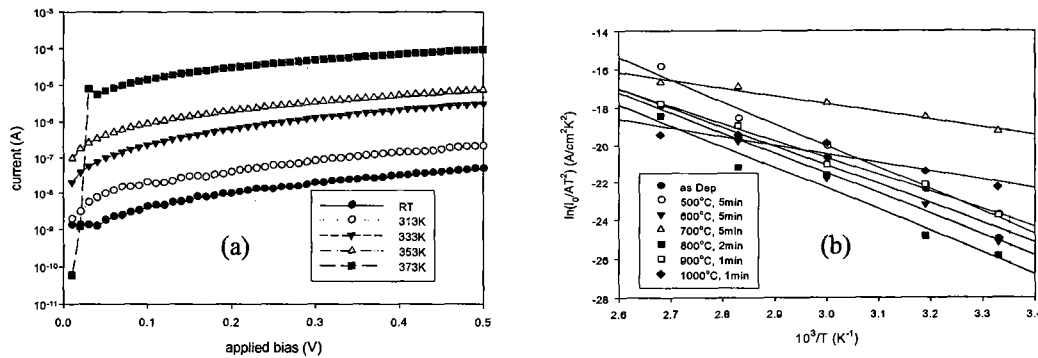


Fig. 1 (a) Measured I-V-T curves of the Ti/p-GaN diode annealed at 500°C range 300-373K to obtain saturation current, I_o . **(b)** Activation energy plots method in extracting barrier heights and effective Richardson coefficients from I-V-T data for different annealing temperature of Schottky contact on p-GaN.

As usual, A is the contact area, k is the Boltzmann's constant, T is the absolute temperature, Φ_B is the barrier height and A^* is the effective Richardson coefficient. The theoretical value of A^* can be calculated using $A^* = 4\pi m^* q k^2 / h^3$, where h is Planck's constant and $m^* = 0.80m_o$ is the effective hole mass for GaN [10,11]. As shown in Fig. 1(a), the plot of $\ln I$ vs V will give a straight line with a slope of $q/\eta kT$, and the intercept with y-axis will yield I_o . The barrier heights of the Schottky diodes were determined from the slope of $\ln(I_o/AT^2)$ vs $1/T$ base on Eq. (3), as shown in Fig. 1(b).

The Schottky barrier height and effective Richardson constants were first extracted using modified Norde Plot [4] and activation energy plot of the measured I-V-T data. Use of either type of plot allows for the independent determination of barrier heights and effective Richardson coefficients. Determination of these parameters with the modified Norde plot method involves plotting the forward-biased I-V-T data as FI vs V where the function $F1$ is defined as:

$$F1 = (qV/2kT) - \ln(I/T^2) \tag{4}$$

Where q is the elementary charge, k is the Boltzmann's constant, and T is the measurement temperature. A typical $F1$ vs V plot for a Ti Schottky diode is shown in a Fig. 2(a) for measurement temperature ranging from 300-373K. Each curve contains a minimum $F1$ or $F1_m$, which is recorded along with the corresponding current, I_m . $F1_m$ and I_m are then used in the left-hand side of Eq. (2) given by

$$2F1_m + (2-\eta) \ln(I_m/T^2) = 2 - \eta [\ln(AA^{**}) + 1] + (q \eta \Phi_{B0}/kT) \tag{5}$$

where Φ_{B0} is the zero-bias Schottky barrier height, and η is the ideality factor. The values of Φ_{B0} and A^{**} are extracted from the slope and y-intercept, respectively, of the $2F1_m + (2-\eta) \ln(I_m/T^2)$ vs qkT plot or modified Norde plot. The modified Norde plots for typical diode of each deposited metal are shown in Fig. 2(b).

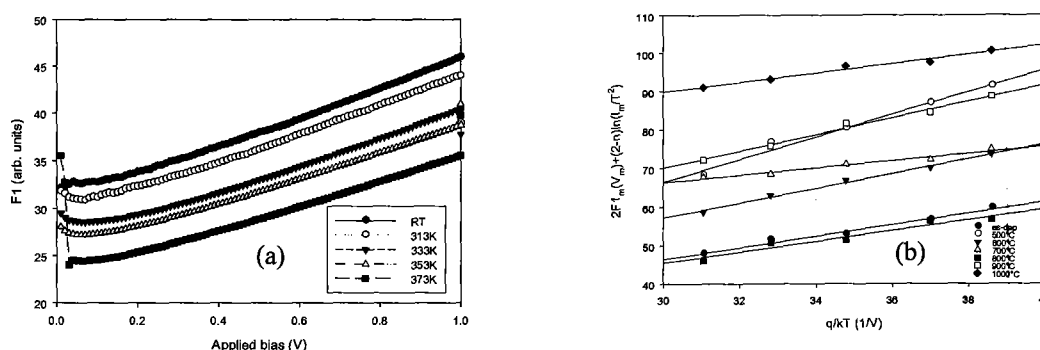


Fig. 2 Plots used in the modified Norde plot method in extracting barrier heights and effective Richardson coefficients from data. (a) $F1$ vs applied bias (V) plot of a typical Ti diode for a series of temperatures annealed at 500°C , (b) $2F1_m(V_m) + (2-\eta) \ln(I_m/T^2)$ vs q/kT plots for Ti on p-GaN, as-deposited and annealed at $500\text{-}1000^\circ\text{C}$.

The built-in potential is

$$V_i = \Phi_B/q - V_n \tag{6}$$

Where

$$V_n = (E_F - E_V)/q = (kT/q) \ln(N_V/N_A) \tag{7}$$

The effective intensity of states in the valence band for Wurtzite crystals is given by [12]

$$N_V = 8.9 \times 10^{15} \times T^{3/2} (\text{cm}^{-3}) \tag{8}$$

At $T=300\text{K}$, $N_V = 4.62 \times 10^{19} \text{ cm}^{-3}$ and $V_n = 0.1143 \text{ eV}$. Thus, the built-in potential could be calculated. The measured value of the SBHs were stated in Table 1 for chosen annealing temperatures on Ti/p-GaN.

To predict the behavior of p-GaN, we try to obtain the electron affinity χ of the semiconductor for a Schottky barrier, which is related to the work function of the metal, Φ_B and band-gap, as state in Eq. (1). This relationship is not so simple in practice because of charges that often exist at the junction caused by surface states, metal-induced gap states or chemical reaction at the interface. Taking $\Phi_m = 4.33\text{eV}$ for Ti [13] and $E_g = 3.39\text{eV}$ [12], as-deposited Φ_B as standard, the electron affinity is determined to be $\chi = 1.81\text{eV}$. This value is factor of 2 lower than estimated $\chi = 4.1\text{eV}$ [12]. This may indicates that the nature behavior of p-GaN which usually exhibit leaky I-V characteristics, making the measurement of SBHs difficult using I-V and C-V methods [14].

The value of A^{**} was found to vary between each metal. Ignoring optical phonon scattering and quantum mechanical reflection/tunneling, the theoretical value of A^{**} is determined to be $(103.8 \text{ Acm}^{-2}\text{K}^{-2})$ [10] based on an effective hole mass of $m^*=0.80m_0$. However, an ideal A^{**} of $26.4 \text{ Acm}^{-2}\text{K}^{-2}$ for n-GaN, and experiments have shown that A^{**} does not agree with this ideal value [15-17]. As a result, the range of measured A^{**} for various annealing temperatures to Ti/p-GaN, which varies over 2 order of magnitude and even more from the theoretical value, are then also expected cannot be explained in terms of quantum or phonon scattering [18]. The differences in A^{**} between metals suggests that the characteristics of the metal, such as metal work function or room-temperature diffusion/intermixing of metal into GaN, may affect the nature of the metal/GaN interface [18]. Error in the determination of A^{**} can also arise from the extrapolation over a narrow range of measurement data to the y-axis in the activation energy plot. Two aforementioned approaches involving I-V-T measurements were thus utilized in determining SBH because the value of A^{**} is not required to obtain SBH.

Table 1 The measured Schottky parameter for Ti/p-GaN at different annealing temperatures.

Annealing temperature	Ideality factor, η	Activation energy plots		Modified Norde plot		Tunneling probability, E_{oo} (eV)	Built-in potential, V_i (eV)
		Φ_B (eV)	A^{**} ($\text{Acm}^{-2}\text{K}^{-2}$)	Φ_B (eV)	A^{**} ($\text{Acm}^{-2}\text{K}^{-2}$)		
As-Deposited	1.82	0.87	1.192×10^4	0.82	1599.56	0.0524	0.76
500°C, 5min	2.85	1.00	2.79×10^6	1.02	3.18×10^6	0.0820	0.89
600°C, 5min	2.23	0.89	310.04	0.85	2704.1	0.0578	0.78
700°C, 5min	2.71	0.40	0.0228	0.38	0.00562	0.0731	0.29
800°C, 2min	1.69	0.96	59.22×10^3	0.83	494.37	0.0546	0.85
900°C, 1min	2.78	0.79	775.96	0.77	275.53	0.0721	0.68
1000°C, 1min	3.28	0.51	0.090	0.37	0.000205	0.1057	0.40

Note: The values shown are averages of at least 8 diodes of each metal.

The standard deviation of SBHs and ideality factor for each annealing temperature respectively are 0.05eV and 0.06.

The thermionic emission model in Eq. (3) predicts a $1/kT$ dependence of a linear region of the $\ln I$ versus V curves, in contrast to the parallel slopes of the $\ln I$ - V curves shown in Fig. 1 (a). This parallel behavior of the $\ln I$ - V curves is commonly observed for carrier transport with a dominant tunnel component [19,20]. It is appropriate to analyze the I-V characteristics using a tunneling model [21]:

$$I \sim AA^*B \exp \{-q \Phi_B / E_{oo}\} \exp \{qV / E_{oo}\} \quad (9)$$

$$E_{oo} = q\hbar \sqrt{(N_A / m^* \epsilon_s)} / 2 \quad (10)$$

Where N_A is the acceptor concentration, ϵ_s the dielectric constant of semiconductor, B a parameter related to the temperature and the Fermi level in the semiconductor. The E_{oo} is a characteristic energy related to the tunneling probability. The defect-assisted tunneling across the barrier would lead to an E_{oo} value larger than that calculated by Eq. (10) based on acceptor concentration alone [20]. According to Eq. (9), the slope of $\ln I$ - V curves is independent of temperature. The parallel shifts of I-V curves were due to the temperature-dependent pre-exponential factor, B . Furthermore, the slope of the $\ln I$ versus V linear region yields the value of E_{oo} . Based on the tunneling model and the experimental results, we deduced E_{oo} values of each annealing temperature as stated in table I. According to Morkoc et al. [22], for $kT / E_{oo} \approx 1$ a mixture of thermionic, thermionic field emission and tunneling mechanisms is observed. Therefore, the deduced values is likely to contain a tunneling component caused by defect states located in the near surface region of the semiconductor in addition to the acceptor concentration (N_A) expressed in Eq. 10.

An ideality factor, $\eta > 1$ could be ascribed to interface states at a thin oxide between the metal and semiconductor [23], or generation-recombination currents within the space region [13].

4 Conclusion

From experimental results such as the ratio of $kT/E_{00} \approx 1$, large A^{**} and large deviation of X from general value indicate that the mixed thermionic emission with thermionic field emission are most possible to be occurred as current transport mechanism. Leaky behavior also expected for our diodes. Beside, Φ_B could be improved by heat treatment with appropriate annealing temperatures and duration.

Acknowledgements This work was conducted under an IRPA RMK-8, Strategic Research grant (MO-STI). The support from Universiti Sains Malaysia is gratefully acknowledged.

References

- [1] F. A. Ponce, and D. P. Bour, *Nature (London)* **386**, 351 (1997).
- [2] M. S. Shur and M. A. Khan, *MRS Bull.* **22**, 44 (1997).
- [3] M. A. Khan, J. N., Kuzma, A. R. Bhattarai, and D. T. Olson, *Appl. Phys. Lett.* **62**, 1786 (1993).
- [4] D. K. Schroder, *Semiconductor material and devices characterization* (New York: John Wiley & Sons, 1998) p207.
- [5] T. Mori, T. Kozawa, T. Ohwaki, Y. Taga, S. Nagai, S. Yamasaki, S. Asami, N. Shibata, M. Koike, *Appl. Phys. Lett.* **69**, 3537, (1996).
- [6] K. A. Rickert, A. B. Ellis, J. K. Kim, J. -L. Lee, F. J. Himpsel, F. Dwikusuma, T. F. Kuech, J. *Appl. Phys.* **92**, 6671, (2002).
- [7] I. Adesida, A. C. Schmitz, A. T. Ping, and M. A. Khan, presented at the Spring MRS Meeting, San Francisco. C. A. April, (1996).
- [8] K. N. Lee, X. A. Cao, C. R. Abernathy, S. J. Pearton, A. P. Zhang, F. Ren, R. Hickman, J. M. Van Hove, *Solid-State Electronics* **44**, 1203-1208, (2000).
- [9] S. M. Sze, *Physics of Semiconductor Devices*, 2nd edition (John Wiley & Sons, New York), 245, (1989).
- [10] *D. Donoval, V. Kulikov, P. Beño, J. Racko, ASDAM 2002.*
- [11] J. I. Pankove, S. Bloom, and G. Harbeke, *RCA Rev.* **36**, 163 (1975).
- [12] M. E. Levinshtein, S. L. Rumyantsev, M. S. Shur, *Properties of advanced semiconductor materials*, (A Wiley-Interscience publication), 2001.
- [13] E. H. Rhoderick and R. H. Williams, *Metal-Semiconductor Contacts* (Clarendon Press, Oxford) 2nd edition, 1988.
- [14] H. Ishikawa, S. Kobayashi, Y. Koide, S. Yamasaki, S. Nagai, J. Umezaki, M. Koike, and M. Murakami, *J. Appl. Phys.*, **81**, pp. 1315-1322, 1997.
- [15] P. Hacke, T. Detchprohm, K. Hiramatsu and N. Sawaki, *Appl. Phys. Lett.*, **63**, 2676, 1993.
- [16] A. T. Ping, A.C. Schmitz, M. A. Khan and I. Adesida, *Electron. Lett.* **32**, 68, 1996.
- [17] J. D. Guo, M. S. Feng, R. J. Guo, F. M. Pan and C. Y. Chang, *Appl. Phys. Lett.*, **67**, 2657, 1995.
- [18] C. Schmitz, A.T. Ping, M. Asif Khan, Q. Chen, J. W. Yang. And I. Adesida, *Journal of Electronic Materials*, **27**, 4, 1998.
- [19] J. M. Andrews, *J. Vac. Sci. Technol.*, **11**, 972, 1974.
- [20] S. M. Sze, *Physics of semiconductor Devices*, 2nd ed. (Wiley, New York, 1981), chapter 5.
- [21] L. S. Yu, Q. Z. Liu, D. J. Qiao, S. S. Lau, and J. M. Redwing, *J. Appl. Phys.*, **84**, pp2099-2104, 1998.
- [22] H. Morkoc, *Nitride Semiconductors and Devices* (Berlin: Springer, 1999), p203.
- [23] J. H. Werner, A. F. J. Levi, R. T. Tung, M. Anzlower and M. Pinto, *Phys. Rev. Lett.* **60** (1988) 53.